

STUDY OF DISCONTINUITIES LOCALIZATION IN ROCK USING ACOUSTIC EMISSION

M. CH. REYMOND

Unité Mixte Centre National de la Recherche Scientifique
Laboratoire Central des Ponts et Chaussées
(2 Allée Kepler, 77420 Champs sur Marne, France)

A. JAROSZEWSKA

Institute of Fundamental Technological Research
Polish Academy of Sciences
(00-049) Warszawa, Świętokrzyska 21)

A slow failure process of Rothbach sandstone and schist from Beringen in Belgium was examined, with particular attention to fault plane localization. The samples of rock were tested under uniaxial compressive stress. Acoustic emission and strain were measured during loading. The data obtained show that the localization threshold of fault plane occurred at stress levels with substantial variability relative to the ultimate strength, depending on the degree of dilatancy and homogeneity of rock under test.

1. Introduction

Deformation process and threshold of localization of strains i.e. of eventual fault plane, under uniaxial compressive stress of rock until macroscopic failure, have been investigated using acoustic emission (AE) and extensometric techniques.

Evolution of a microcrack was studied during various stages of failure process. Special attention was given to its localization to enable extrapolation of the AE data obtained in the final loading stage in laboratory, to field conditions. The experimental results obtained by TROMBIK and ZUBEREK [1] and BRADY *et al.* [2] show substantial amount of similarities between the seismic data from the surface observations and those obtained in laboratory in failure process of rock. These similarities seem to indicate that the examined phenomena in spite of significant difference in the scale, have much in common.

2. Specimen materials

The measurements were performed on laboratory samples of Rothbach sandstone and schist from Beringen, Belgium.

The Rothbach sandstone is a brittle rock, of isotropic structure, with mean porosity of 18%. Its mean compressive strength is between 40 and 50 MPa and mean longitudinal elastic wave velocity amounts to 2680 m/s.

The tested schist is a dense anisotropic, layered rock with layer planes inclined 5° to 25° . Its mean compressive strength is between 80 to 99 MPa, while mean longitudinal elastic waves velocity in this rock falls in the range 4500-4800 m/s.

The cylindrical samples 40 mm in diameter and 80 mm in length were used throughout the experiment.

3. Apparatus

3.1. Strain measurement

For strain measurement, the extensometers in the form of a rosette made of three resistance-type strain gauges, with the angles of 120° were attached to the rock samples surface on half of their length. The strain gauges were connected to a bridge and its output to a PC computer. Graphic form of the strain data as a function of applied stress was obtained using Mc Intosh system.

3.2. AE measurement

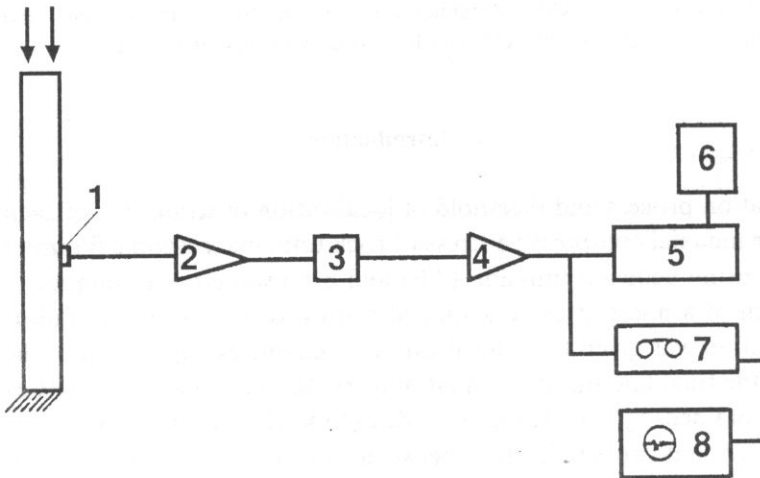


Fig. 1. Block diagram for AE measurement: (1) accelerometer, (2) preamplifier, (3) filter, (4) amplifier, (5) digital counter, (6) printer, (7) magnetic recorder, (8) digital oscilloscope.

The block diagram of the testing equipment for acoustic emission measurement is given in Fig. 1. AE signals were detected by a Bruel & Kjaer accelerometer (1) with sensitivity of 60 mV/g and flat frequency response in the range 2 Hz-20 kHz. The accelerometer was attached to the side surface of the rock samples. Its output was connected through preamplifier (2) to AE monitoring apparatus. The filtered (3) and amplified (4) signals were fed to a digital counter (5) and to a printer (6) and AE count rate was determined above the fixed reference threshold. The AE signals at the output of the amplifier (4) were recorded using a Nagra (7) magnetic tape recorder with frequency response flat in the range 20 Hz-20 kHz. The recorded signals were further processed using a digital oscilloscope (8) for determination of AE cumulative (total) count, maximum frequency spectrum, rise-time of AE signals, their maximum (peak) amplitude and also for determining of the relationship between AE and mechanical parameters i.e. load and strain.

The experimental arrangement as given in Fig. 1 was used for investigation performed in France. The measurements of AE event rate, cumulative (total) number of events and of cumulative peak amplitude were performed in Poland on several samples of the schist. The equipment used in Poland for the AE measurements was principally almost the same as used in France but its frequency range was from 1 kHz up to 100 kHz.

3.3. Loading apparatus

The rock specimens were loaded in a manually-operated hydraulic testing machine to avoid interference of its noises with the AE signals.

4. Experimental procedure

Loading rate effect on rock behaviour under uniaxial compression test was investigated e. g. by HOUPERT [3], SALA [4] and KHAIR [5]. Behaviour characteristic of geologic material is highly affected by the rate of applied stress and heterogeneity of the vertical stress field distribution within the structure. Inhomogeneities and discontinuities in rock which constitute obstacles for the fractures development, generally recognised as "barriers" that usually form the regions of increased strength, are progressively overcome by the propagating fractures. An intervention of these "barriers" is larger with lower loading rate than with higher loading rate. This concept seems to be supported by examination of the rock failure surfaces performed by HOUPERT [3] because under lower loading rate, fracture surfaces were more rough and the fragmentation of rock samples into much smaller pieces was observed. Strength and dynamic behaviour of geologic material are reduced substantially while the AE activity increases under very low rate of applied stress, indicating also larger intervention of structural defects under lower stress rate [5]. The stress rate effect is more pronounced especially if geologic material contains larger number of defects i.e. inhomogeneities and discontinuities.

The process of rock failure in laboratory under very low loading rate is analogous to the failure process of rock mass in situ which usually occurs as a result of very low stress rate. This process is investigated in seismology where a concept of the "barriers" in a sense of the obstacle for a propagating crack was introduced by DAS and AKI [6]. Long term seismological observations usually show an increase of seismicity which precedes occurrence of dynamic rock mass failure [7, 8, 9]. Long term observations show also local rise of the terrain which precedes some of earthquakes indicating higher rate of rock mass displacement i.e. a change of the state of deformation relative to certain more or less long-lasting stable periods. Thus these observations implied performance of the AE laboratory measurements at low loading rate. They also implied concurrent measurements of both AE and strain with the aim to use the data and the relationship between them in predicting of the occurrence of dynamic seismic phenomena [10, 11, 12, 13].

In the present experiment the rock samples were tested under constant loading rate of 170 N/s in 1 min intervals. After each 1 min increment of the load it was kept constant up to the total decay of acoustic emission.

5. Sandstone data analysis

5.1. Strain analysis

The dependence of relative longitudinal (axial) strain ε_1 , transversal strain ε_2 and volumetric strain $\varepsilon_v = \varepsilon_1 + 2\varepsilon_2$ on axial stress σ , is given in Fig. 2a for a sandstone sample. Several stages of deformation can be distinguished in the graph:

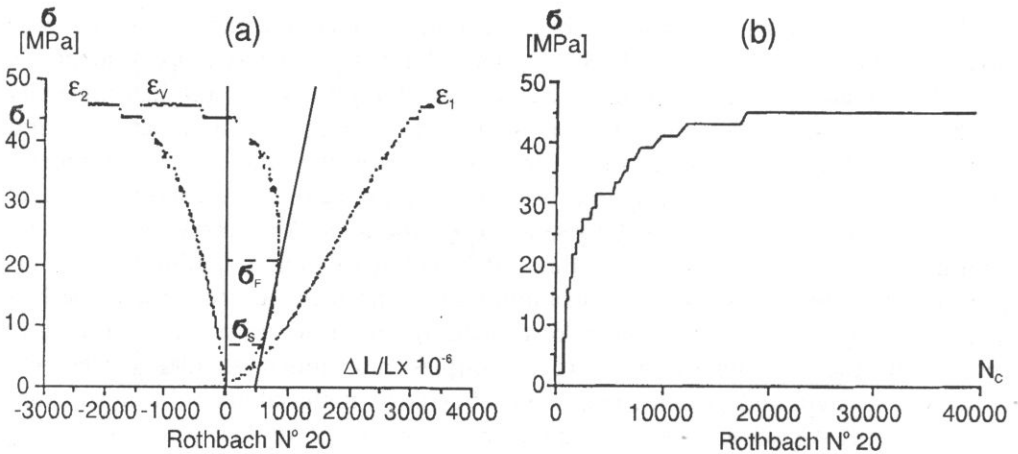


Fig. 2. Dependence of: (a) longitudinal strain ε_1 , transversal strain ε_2 , volumetric strain ε_v and (b) cumulative count N_c of acoustic emission on stress σ for sandstone.

- stage in which defects do not develop; in case of primarily fissured rock it corresponds to closing of the pre-existing microfissures which can be observed on curves ε_1 and ε_v as a convexity towards the strain axis; limit of compactness stage corresponds to stress σ_s .
- stage of linear-elastic deformation, characterised by linearity of all stress-strain relationships; this phase is limited by the threshold of microcracking σ_F .
- stage of stable microcracks propagation; in this phase, above the threshold σ_F , a propagation of pre-existing microdefects begins and new microcracks develop resulting in the effect of the so called microdilatancy (or relative dilatancy); stress-transversal and volumetric strain plots loose their linearity, and growth of transversal strain occurs; relative sample volume ($\frac{\Delta v}{v} = \varepsilon_1 + 2\varepsilon_2$) decreases whilst longitudinal strain characteristic remains linear.
- stage of unstable, self-supporting microcracks propagation, observed above stress σ_L , characterised by nonlinearity of all the stress-strain curves; substantial increase of ε_2 and increase of absolute sample volume, i.e. characterised by effect of dilatancy (absolute dilatancy or macrodilatancy).

A macroscopic failure occurs as a result of bifurcation and localization of strains in a limited region that constitutes a "nucleus" of approaching failure, usually in a vertical spalling manner or in a shear mode [5]. Failure occurs at stresses higher than the threshold at which the damage begins to localize.

HOUPERT *et al.* [14] characterise stress – volumetric strain relation for brittle rock fracture by the ratio of the surface between stress axis σ and the volumetric strain curve ε_v , to the surface between stress axis σ and the linear extrapolation of the linear part of the volumetric strain curve (which corresponds to the volumetric strain curve for the same but not dilatant material), Fig. 2a. According to the authors [14] this ratio properly defines a relative value of dilatancy.

A different representation of stress and strain curves, namely as a function of loading time, Fig. 3, confirms existence of the discussed stages of the sandstone deformation process.

5.2. Analysis of AE in sandstone

Simultaneous analysis of strain and of acoustic emission, i.e. of cumulative count N_c as a function of compressive stress, Fig. 2b and count rate \dot{N}_c as a function of loading time t , Fig. 3, confirms existence of the four stages of the sandstone failure process, namely:

- compactness stage in which AE is mostly due to the friction produced by closing of the pre-existing fissures and which occurs up to approximately 10% of the ultimate strength σ_M ,
- linear-elastic deformation stage with low AE level that is observed up to approximately 30% of σ_M ,

- between 30% and 60% of σ_M , the curve of volumetric deformation indicates an effect of microdilatancy; this effect is accompanied by stable increase in AE which begins near the threshold of microcracking σ_F ,
- between 60% and 80% of σ_M , AE activity increases which corresponds to the effect of dilatancy; on average at about 70-80% σ_M a marked increase of AE is observed which indicates the beginning of the heterogeneous strains distribution that is the beginning of the process of their localization.

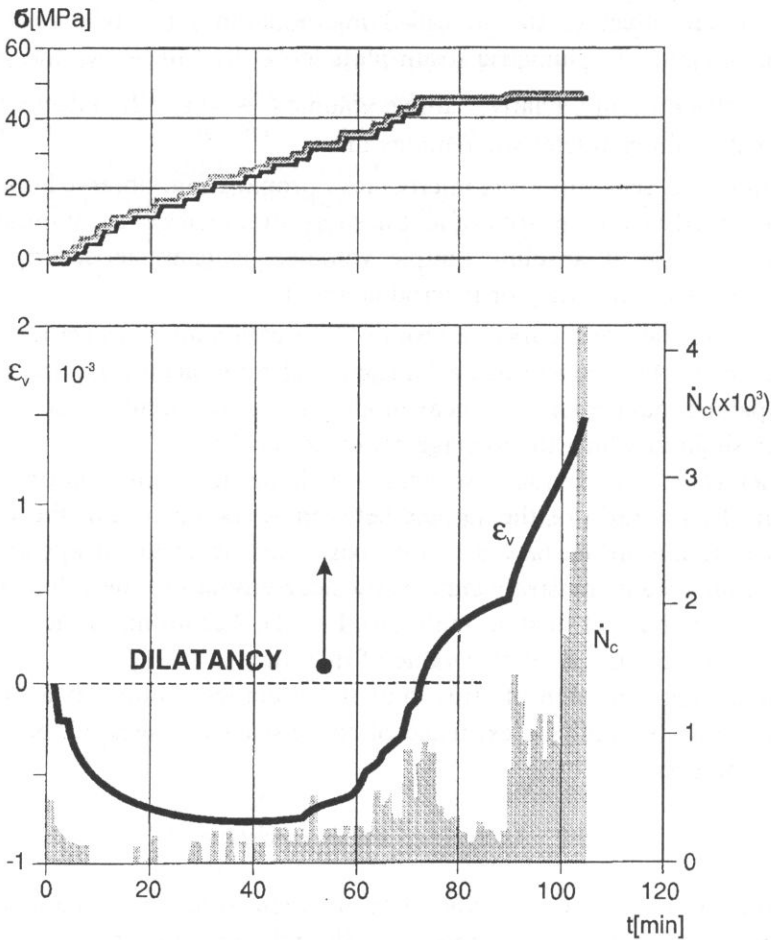


Fig. 3. Dependence of stress σ , volumetric strain ϵ , and AE count rate \dot{N}_c on loading time t for sandstone.

In general the AE cumulative count as a function of stress observed for the sandstone, corresponded to "Mogi" type, as presented in Fig. 4, [15].

Frequency spectrum analysis. A spectrum analysis was performed for the AE recorded signals and the maximum spectra were determined for the successive stages of deformation. The results obtained indicate evolution of the AE frequency spectra as

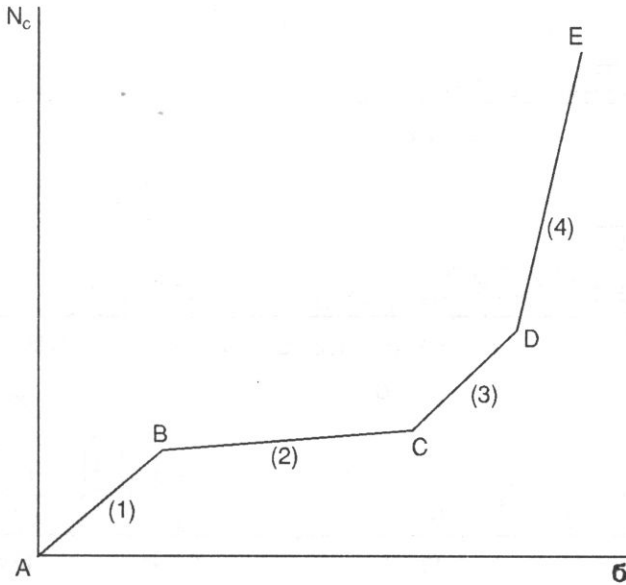


Fig. 4. AE cumulative number of events or count as dependent on stress or loading time characteristic for "Mogi" type of rock behaviour: (1) closing of fissures, (2) linear-elastic deformation, (3) stable propagation, (4) unstable propagation of microcracks.

a function of load applied to the sample [16, 17]. The results of AE spectrum analysis can be used for determining of the sample deformation stages in the failure process of rock. Characteristic maximum frequency spectra of AE for various stress levels are presented in Fig. 5 where:

a – corresponds to a stage of closing of pre-existing microfissures; relatively low frequency spectral components are observed,

b, c, d – correspond respectively: to the initiation of microcracks, to the growth of the microcracks grid density and to their coalescence: progressive upward shift of the spectral components is observed,

e – corresponds to microcracks localization, since for 70-80% of σ_M , a shift of the spectrum towards lower frequencies and decrease of dominant frequency from 8 kHz for the spectrum "d", to 2 kHz for the spectrum "e" is observed; this effect indicates an increase of the AE source dimensions.

Maximum amplitude and rise-time. A relationship between peak amplitude of AE signals and their rise-time was determined using a digital storage oscilloscope. This relationship is given in Fig. 6 for three sandstone samples. Each data point in the graph is a mean of 10 measurements for each sample. The results obtained indicate smaller rise-times for larger amplitudes of AE signals. The data are in agreement with the model of behaviour of a concrete described by REYMOND [18] for which smaller rise-times corresponded to AE signals of larger energy. With the increase of stress level and consequently with the increase of energy in AE signals, these signals

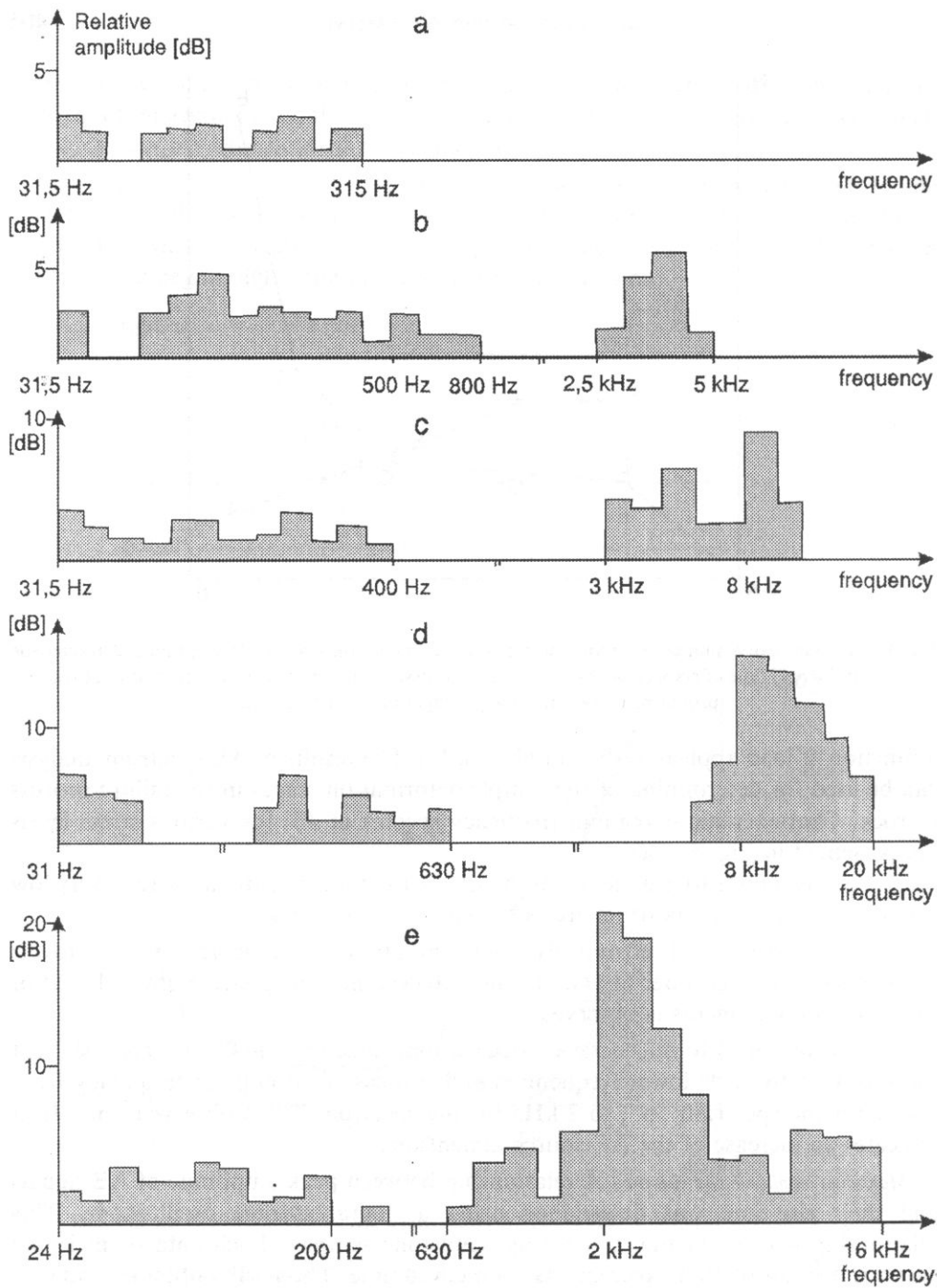


Fig. 5. Maximum AE frequency spectra of sandstone for various deformation stages: a, b, c, d, e.

had smaller rise-times and thus gained spectral components of higher frequency. These experiments [18] however, were carried out below the threshold of strains localization and therefore the effect of lowering of AE signal frequencies in the final stage of loading were not observed.

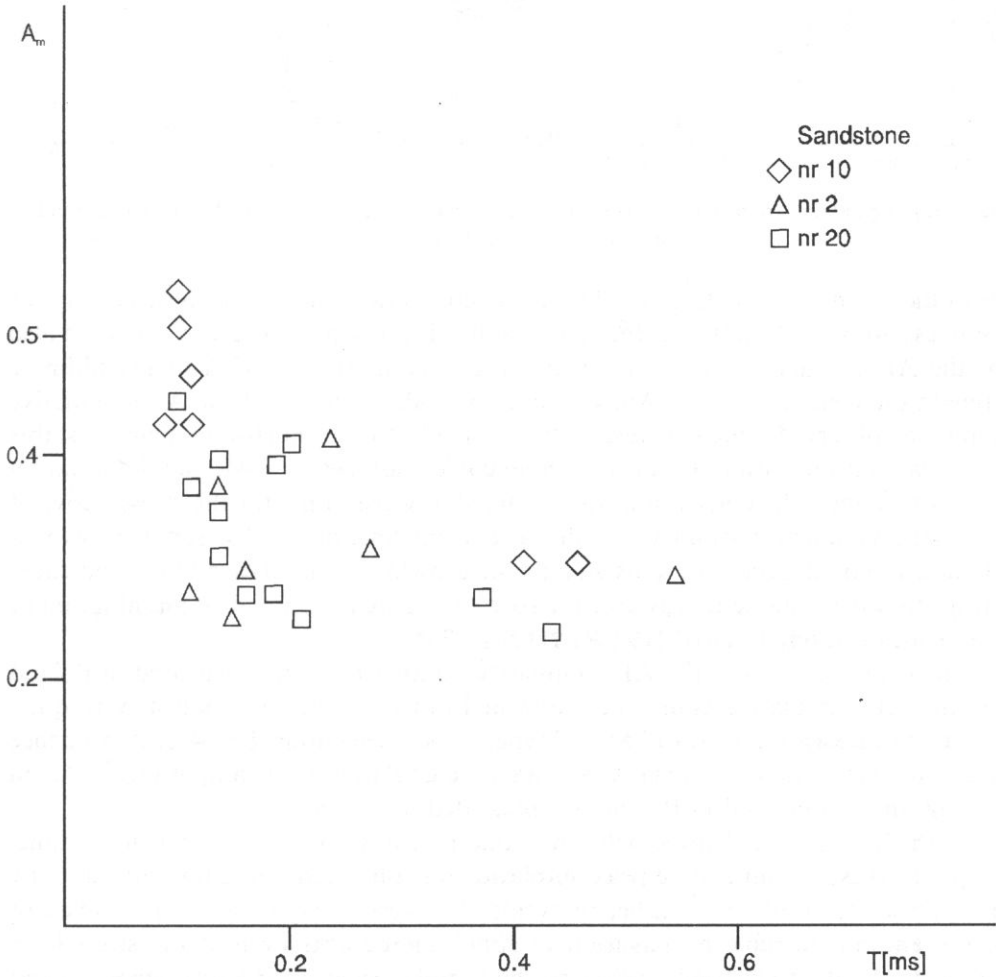


Fig. 6. Relations between maximum amplitude A_m and rise-time T of AE signals in sandstone.

6. Schist data analysis

6.1. Analysis of strain and AE

Strain curves for schist in a process of compressive load show a linear character of these functions, Fig. 7a. An effect of dilatancy was practically absent in the tested samples. The samples deformed linearly almost in the whole range of the stress level

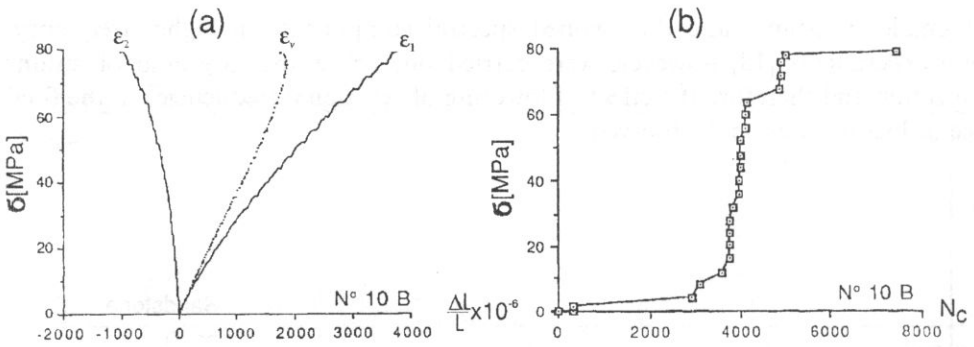


Fig. 7. (a) Logitudinal strain ϵ_1 , transversal strain ϵ_2 , volumetric strain ϵ_v , and (b) AE cumulative count N_c in schist as a function of stress σ .

up to the ultimate strength limit. The volumetric strain curve lost linearity only for the stress above 90% of the ultimate strength. Linear dependence was observed also for the AE cumulative count up to the stress amounting to 85% of the ultimate strength on average, Fig. 7b. Above this value stable increase of the AE cumulative count was observed which corresponded probably to the short-term stage of stable microcracks propagation. In this region no correlation between AE and deformation plots was found. The correlation was observed however, only for the stress above of which the volumetric strain curve declined from linearity and a rapid growth of cumulative count occurred. This significant growth of cumulative count indicated a transition from stable to unstable microcracks propagation and so an initiation of strains localization, THIMUS [19], REYMOND [20].

The characteristics of the AE cumulative number of events measured in Poland and the AE cumulative count measured in France on the same schist were quite similar. Both corresponded to "Mogi" type of rock behaviour, Fig. 4. A dependence of cumulative number of events N_c and of cumulative peak amplitude $\sum A_m$ on loading time t , obtained in Poland are presented in Fig. 8.

Both the curves had principally the same plot however, for some loading time, a rapid increase of cumulative peak amplitude was observed, preceding substantially an increase of cumulative number of events. This result may indicate an increase of energy and an unstable propagation of some microcracks even at the stress level corresponding to 15 min of loading, in the sample tested. In the final stage of load after relatively short period of acoustic „quiescence”, a rapid increase of cumulative number of AE events and of cumulative peak amplitudes, for stress about 90% of the ultimate strength, was observed indicating an initiation of strains localization. The data on maximum amplitude show that it is a "sensitive" indicator of rock behaviour under load and is a parameter closely correlated with AE source mechanism.

The evolution of AE frequency spectrum and the dependence of maximum amplitude of AE signal on its rise-time, have qualitatively the same character for the schist as for the sandstone tested.

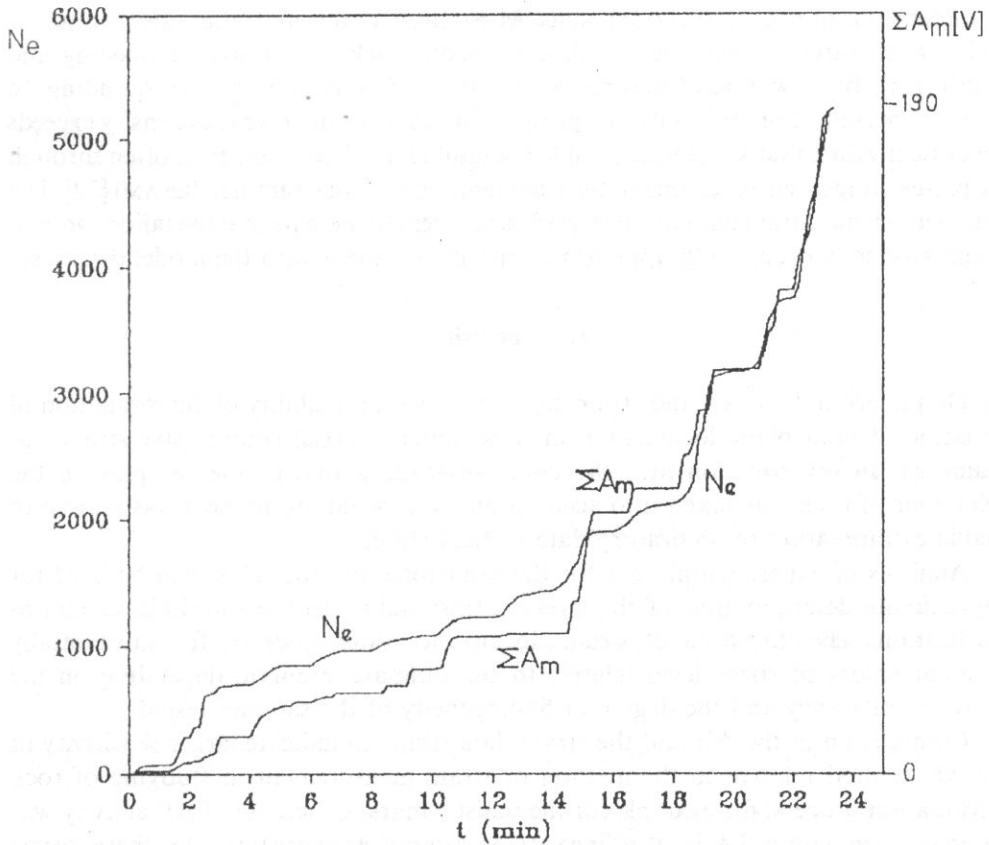


Fig. 8 Cumulative number of events N_e and cumulative maximum amplitude ΣA_m of acoustic emission in schist as a function of loading time t .

7. Discussion

A model of the failure process of inhomogeneous materials is generally, with certain approximation, in agreement with Griffith's theory and stems from the assumption that cracks propagate chiefly by increasing in length. In this model an initiation of microcracks is recognised, occurring above the threshold of microcracking and next a stable and an unstable propagation of cracks [21]. To this model such materials as glass, ceramics and some metals seem to suit well, whereas propagation of cracks by their elongation does not seem to be compatible with mineralogical data and with experimental observations of the behaviour of inhomogeneous rock. Actually, a failure of inhomogeneous rock seems to result from the growth in number (density) of elementary microcracks and consequently from the expansion of the dense grid of these microcracks with the dimensions determined

by dimensions of rock grains or crystals. Most often a grid of primary discontinuities and microfissures pre-existing in inhomogeneous rock is a source of opening and multiplying of new microfractures above the threshold stress corresponding to microcracks initiation. It is only just prior to failure when microcracks density exceeds the critical value, that some microcracks in a limited local area coalesce, often through the pre-existing fissures, leading to the fragmentation of rock sample, PERAMI [22]. The obtained AE and strain data for the tested schist seem to indicate that the failure process in this case may occur, with approximation, in agreement with the model discussed.

8. Conclusion

On the grounds of AE and strain characteristics a possibility of determination of initiation of fault plane localization in rock under uniaxial compressive stress was examined. In investigation also the effect of loading rate of the samples on the behaviour of rock was taken into account and a slow failure process was chosen to enable extrapolation of laboratory data to field studies.

Analysis of experimental data for the sandstone and the schist can be used for approximate determination of the stress corresponding to the threshold of strains localization. The threshold of strains localization was observed for substantially different values of stress level relative to the ultimate strength, depending on the degree of dilatancy and the degree of homogeneity of the samples tested.

Comparison of the AE and the strain data seems to indicate larger sensitivity of the AE method relative to the method of strain measurement in studying of rock deformation process; for example for the schist a marked increase of AE activity was observed even within the limit of linearity of strain characteristics. This thesis seems to be justified since the AE signals are generated by the discrete local material instabilities while the strain characteristics result from averaged data for the whole sample. The present results are in agreement with the data obtained by THIERCELIN [23] who reported the microcracks initiation thresholds for some rocks as determined by AE, to occur at lower stresses than the thresholds determined on the grounds of strain measurements.

Acknowledgements

The authors wish to express their thanks to Mr F. MARTINEAU, Unité Mixte CNRS-LCPC Paris, for technical co-operation and to professor J. F. THIMUS, Université Catholique de Louvain, for supplying of the rock samples used in the experiments.

References

- [1] M. TROMBIK, and W. ZUBEREK, *Microseismic research in Polish coal mines*, Proc. 1st Conf. AE/MS Act. Geol. Struct. Mat., Trans Tech Publications, Clausthal, Germany 1975, p. 183-187.

- [2] B. T. BRADY, *An investigation of the scale invariant properties of failure*, Int. J. Rock Mech. Min. Sci. Geomech. Abstr., 14, 121-126 (1977).
- [3] R. HOUPERT, *Le role du temps dans le comportement à la rupture des roches*, C.R. 3 Congr. Internat. Mec. Roches, Denver, 2 et A, 1974, p. 325-329.
- [4] Ph. SALA, *Etude experimentale de la fissuration et de la rupture des roches par émission acoustique*. Application à l'étude de la sismogenese, Thèse Dr Ing, Université de Grenoble 1982, p. 166.
- [5] A. W. KHAIR, *Stress rate effect on A.E.*, Proc. 5th Conf. AE/MS Act. Geol. Struct. Mat., Trans Tech Publications, Clausthal, Germany 1995, p. 29-43.
- [6] S. DAS and K. AKI, *Fault plane with barriers; a versatile earthquake model*, J. Geoph. Res., 82, 5658-5670 (1977).
- [7] C. B. RALEIGH, G. BENNETT, H. CRAIG, T. HANKS, P. MOLNAR, A. NUR, J. SAVAGE, C. B. SCHOLZ, R. TURNER, and F. WU, *The prediction of the Haicheng earthquake*, EOS Trans. Am., Geoph. Union, 58, 236-272 (1977).
- [8] M. WYSS, and W. H. K. LEE, *Time variations of the average earthquake magnitude in Central California*, Proc. Conf. Tectonic Problems of the San Andreas Fault System, Stanford Univ., Publ. Geol. Sci., 13, 1973, p. 24-42.
- [9] B. T. BRADY, *Anomalous seismicity prior to rock bursts; Implication for earthquake prediction*, Pageoph, 115, 357-374 (1977).
- [10] T. HIRATA, *Omori's power law aftershock sequences of microfracturing in rock fracture experiment*, J. Geoph. Res., 92, B7, 6215-6221 (1987).
- [11] R. REVALOR, J. P. JOSIEN, J. Ch. BESSON, A. MAGRON, *Seismic and seismoacoustic experiments applied to the prediction of rockbursts in French coal mines*, University of Minnesota USA 1988.
- [12] K. MISHIHIRO, *Study on estimating initial stress and predicting failure in rock masses by AE*. Rock at great depth., Maury and Fourmaintraux, Balkema, Rotherdam, ISBN 90619754 (1989).
- [13] H. R. HARDY, Jr., *A review of international research relative to the geotechnical field application of AE/MS techniques*, Jour. Acoust. Emission, 8, 4, 65-91 (1989).
- [14] F. HOMAND-ETIENNE, R. HOUPERT, *Le comportement dilatant des roches*, Laboratoire de Geomecanique-Ecole de Geologie de Nancy (1976).
- [15] A. JAROSZEWSKA, *Acoustic emission in geologic materials*, in Acoustic Emission; Sources, Methods, Applications (in Polish), Pascal Publications, Warsaw 1994, p. 323-352.
- [16] M. C. REYMOND, and A. JAROSZEWSKA, *Study of the AE frequency spectra of some rocks*, Archives of Acoustics, 14, 1-2, 97-109 (1989).
- [17] A. JAROSZEWSKA, M. C. REYMOND, *Characteristic features of AE in some rocks*, Proc. 5th Conf. AE/MS Act. Geol. Struct. Mat., Trans Tech Publication, Clausthal, Germany 1995, p. 19-27.
- [18] M. C. REYMOND, *Signature acoustique du béton*, 11 Congrès International d'Acoustique, Revue Acoust., hors serie, 5, 115-118 (1983).
- [19] J. F. THIMUS, O. MOUSTACHI, J. BERGUES, M. C. REYMOND, F. MARTINEAU, *Contribution de l'émission acoustique à l'étude de la fissuration des roches*, Colloque R. Houpert, Nancy 1992, p. 229-232.
- [20] M. C. REYMOND, J. F. THIMUS, and Ph. LINZE, *Acoustic emission characteristics of schists and sandstones*, British J. Non-Destructive Testing, 33, 4, 183-185 (1991).
- [21] Z. T. BIENIAWSKI, *Mechanism of brittle fracture of rock*. Theory of the fracture process, Int. J. Rock Mech. Min. Sci., 4, 395-430 (1967).
- [22] R. PERAMI, *Influence de la microfissuration thermique des roches sur leurs proprietes en compression*, Structure et Comportement Mécanique des Geomateriaux, Colloque R. HOUPERT, Nancy 1992, p. 77-86.
- [23] M. THIERCELIN, *Application de l'émission acoustique à l'étude de la fissuration et de la rupture des roches*, Thèse de doctorat, Université de Grenoble 1980.